CrossMark

ORIGINAL ARTICLE

EphA4-mediated signaling regulates the aggressive phenotype of irradiation survivor colorectal cancer cells

Priscila Guimarães de Marcondes [1] · Lilian Gonçalves Bastos [1] ·
Julio Cesar Madureira de-Freitas-Junior [1] · Murilo Ramos Rocha [1] ·
José Andrés Morgado-Díaz [1]

Abstract Radiotherapy is widely used for advanced rectal tumors. However, tumor recurrence after this treatment tends to be more aggressive and is associated with a poor prognosis. Uncovering the molecular mechanism that controls this recurrence is essential for developing new therapeutic applications. In the present study, we demonstrated that radiation increases the EphA4 activation level of the survivor progeny of colorectal cancer cells submitted to this treatment and that such activation promoted the internalization of a complex E-cadherin-EphA4, inducing cell–cell adhesion disruption. Moreover, EphA4 knockdown in the progeny of irradiated cells reduced the migratory and invasive potentials and metalloprotease activity induced by irradiation. Finally, we demonstrated that the cell migration and invasion potential were regulated by AKT and ERK1/2 signaling, with the ERK1/2 activity being dependent on EphA4. In summary, our study demonstrates that these signaling pathways could be responsible for the therapeutic failure, thereby promoting local invasion and metastasis in rectal cancer after radiotherapy. We also postulate that EphA4 is a potential therapeutic target for colorectal cancer treatment.

Keywords EphA4 receptor · E-cadherin · Signaling pathways · Colorectal cancer · Radiotherapy

✉ José Andrés Morgado-Díaz
jmorgado@inca.gov.br

[1] Cellular Biology Program, Brazilian National Cancer Institute (INCA), 37 André Cavalcanti Street, 5th Floor, Rio de Janeiro, RJ 20230-051, Brazil

Introduction

Colorectal cancer (CRC) is the third most commonly diagnosed cancer in men and second in women worldwide, and these statistics are the same in Brazil [1, 2]. Radiotherapy (RT) is widely used for advanced rectal tumors with the purpose of reducing the tumor size in neoadjuvant treatment. Although preoperative RT reduces the risk of local recurrence in comparison with surgery alone, this confers only a small impact on distant metastasis formation as 30–40 % of the patients will develop metastatic disease [3]. Furthermore, the cumulative incidence of any recurrence at 5 years in patients is still high (around 45 %), and it tends to be more aggressive with invasive metastatic conditions and shorter survival expectancy after preoperative RT [4–8]. Thus, the efficacy of RT is challenged by the local invasion and dissemination of cells that have survived irradiation, which may lead to therapeutic failure. Indeed, distant metastasis has become the major cause of failure in rectal cancer [3]. It is now evident that radiation-induced changes in both the tumor microenvironment and signaling pathways can generate profound cellular effects [9]. For instance, HIF-1α, PI3K/AKT/mechanistic target of rapamycin (mTOR), and mitogen-activated protein kinases (MAPKs) are activated after irradiation [10, 11]. In this context, drugs targeting these signaling pathways with different mechanisms of action directed to a specific tumor type are important to overcome this disease. Clinical trials with these therapeutic purposes have been increased in the last decades, resulting in the regulatory approval of a variety of kinase inhibitors, such as Everolimus (mTOR inhibitor) for kidney tumors and Trametinib (MEK inhibitor) for melanoma [12, 13]. However, no drugs targeting these pathways have been approved for CRC treatment thus far, which reinforces the need to identify new therapeutic targets for this cancer type.

Eph (erythropoietin-producing hepatoma) receptors are the largest receptor tyrosine kinase (RTK) subfamily expressed in the extracellular membrane where it binds to ephrin ligands through its extracellular domain. This interaction enables the cell to recognize signals from the microenvironment and regulate adhesion, migration, and invasiveness [14]. In particular, EphA4 correlates with invasiveness in mammary tumor and glioma models [15, 16]. Moreover, EphA4 expression was correlated with epithelial–mesenchymal transition (EMT) in hepatoma cells [17] and shorter overall survival in pancreatic adenocarcinoma patients [18]. However, EphA4 has never been associated with radioresponse, and its role in CRC remains largely unclear. Furthermore, there have been no clinical studies targeting EphA4 for cancer treatment because its role during tumorigenesis is unknown and because the understanding of this role is challenged by the complexity of the Eph/ephrin system [19].

In a previous study, we demonstrated that the progeny derived from irradiation survivor CRC cells displayed an EMT-like phenotype characterized by the downregulation of E-cadherin and increased migratory and invasive potentials, among other malignant features [20]. However, the signaling pathways supporting this aggressive phenotype remained to be elucidated. Here, we analyzed in vitro the molecular mechanisms underlying this aggressive phenotype that could lead to therapy failure in association with invasion and metastasis after radiotherapy in patients with CRC. Our findings indicate that the progeny of irradiation survivor CRC cells displayed increased EphA4 activation levels, concomitant with adherens junction disorganization and increased cell dispersion, migration, and invasion. Furthermore, we showed that the PI3K/AKT and ERK1/2 pathways, downstream of EPHA4 activation, play a role in the regulation of these events. In conclusion, we postulate that EphA4 could be a new potential therapeutic target for CRC in adjuvant radiotherapy.

Materials and methods

Antibodies

Mouse anti-EphA4 and anti-α-tubulin monoclonal antibodies were purchased from Invitrogen (Carlsbad, CA, USA), and rabbit anti-p-EphA4 (Tyr-602) polyclonal antibody was from ECM Biosciences (Versailles, KY, USA). Rabbit anti-phosphotyrosine was purchased from Millipore (Billerica, MA, USA), and mouse anti-E-cadherin monoclonal antibody was from BD Biosciences (San Diego, CA, USA). Rabbit anti-β-catenin, anti-p-AKT, and anti-AKT antibodies were obtained from Cell Signaling (Danvers, MA, USA). Mouse anti-p-ERK1/2 and anti-ERK1/2 antibodies were purchased from Sigma and mouse anti-GAPDH antibody was from Santa Cruz (Dallas, TX, USA). Goat anti-mouse and anti-rabbit IgG (Alexa Fluor® 488) and goat anti-mouse IgG (Alexa Fluor® 546) antibodies were purchased from Molecular Probes (Eugene, OR, USA). Horseradish peroxidase (HRP)-conjugated anti-mouse and anti-rabbit IgG were purchased from GE Healthcare (Chalfont St. Giles, UK).

Reagents

The 2-(2-amino-3-methoxyphenyl)-4H-1-benzopyran-4-one PD98059 (MEK1 inhibitor) was obtained from Calbiochem (La Jolla, CA, USA). The 2-(4-morpholinyl)-8-phenyl-1(4H)-benzopyran-4-one LY294002 (PI3K inhibitor), 4′,6-diamidino-2-phenylindole dihydrochloride (DAPI), and doxazosin mesilate were purchased from Sigma-Aldrich (Saint Louis, MO, USA).

Cell culture and ionizing radiation treatment

The human colorectal adenocarcinoma cell line HT-29 (HTB-38™) was obtained from the American Type Culture Collection (Manassas, VA, USA). HT-29 cells are moderately differentiated with *BRAF*, *PIK3CA*, *TP53*, *SMAD4*, and *APC* mutations [21, 22]. Cells were maintained in Dulbecco's modified Eagle medium (DMEM; Invitrogen) with 10 % fetal bovine serum (FBS), penicillin G (60 mg/l), and streptomycin (100 mg/l). Cell irradiation and generation of the cell progeny were conducted as previously described [20]. The progeny derived from the non-irradiated cells was named "F1 Control" and that derived from the irradiated cells was named "F1 5Gy."

Pharmacological inhibition of signaling pathways

Control and irradiated cells were maintained as described above and incubated for 24 h with the pharmacological inhibitors LY294002 and PD98059 diluted in dimethyl sulfoxide (DMSO) and stored at −20 °C. Each solution was diluted immediately before each experiment to yield final concentrations of 50 μM (PD98059) and 12 μM (LY294002).

Cell viability assay

HT-29 cells were plated on 96-well dishes (2×10^3 cells) and treated with 1, 10, 20, 30, 50, 70, and 90 μM doxazosin. Cell viability was analyzed 24, 48, 72, and 96 h after treatment by adding 3-(4,5-dimethylthiazol-2-yl)-2,5-diphenyltetrazolium bromide (MTT). Formazan crystals were solubilized with DMSO and the absorbance measured using ELISA reader Spectra Max 190 (Molecular Devices, CA, USA).

Cell extraction and Western blot

Lysate protein extraction and Western blot protocols were described previously [20]. Membranes were incubated with primary antibodies against EphA4 (1:250), α-tubulin (1:1000), E-cadherin (1:5000), β-catenin (1:4000), p-ERK (1:5000), ERK1/2 (1:2000), GAPDH (1:2000), p-EphA4 (1:1000), p-tyrosine (1:1000), p-AKT (1:1000), and AKT (1:1000). Membranes were incubated with secondary antibodies, and protein bands were detected using a chemiluminescence kit (GE Healthcare). Bands were quantified by optical density using LabWorks 4.6 software (Bio-Rad Laboratories, Hercules, CA, USA). When indicated, membranes were washed and reprobed with anti-α-tubulin (1:500) or anti-GAPDH (1:1000) antibodies as a protein loading control.

Phospho-RTK and phosphokinase analysis

The Human Phospho-RTK Array and the Human Phospho-Kinase Array kits were used to analyze phosphorylated proteins in both F1 Control and F1 5Gy according to the manufacturer's protocol (R&D Systems, Minneapolis, MN, USA).

Immunoprecipitation

Equal amounts of total protein (500 μg) from cell lysates were precleared with protein G-sepharose beads (Sigma-Aldrich) and incubated overnight with mouse anti-EphA4 (5 μg). Beads were incubated with protein G-sepharose for 2 h, and the immune complexes were released by boiling for 5 min at 95 °C in Laemmli. Samples were electrophoretically separated using SDS-PAGE as described previously [20] and probed with primary antibody against phosphotyrosine, E-cadherin, or β-catenin and HRP-conjugated secondary antibody against rabbit.

Immunofluorescence microscopy

Control and irradiated cells were grown in glass coverslips until colony formation and processed using immunofluorescence as previously described [20]. After incubating the cells overnight with primary antibodies against E-cadherin (1:300), EphA4 (1:25), or p-EphA4 (1:25), the cells were incubated with the appropriate Alexa Fluor® secondary antibodies (1:500) for 1 h. Then, cells were treated with DAPI (1:1000) for 1 min and mounted using an antifade solution (Life Technologies, Carlsbad, CA, USA, USA). Glass coverslips were visualized in the confocal laser scanning microscope FV10i-O and images were analyzed using the FV10-ASW software (Olympus, Tokyo, Japan).

Super-resolution images were taken using a LSM 710 microscope (Carl Zeiss, Germany) equipped with a PCO Edge sCMOS camera (PCO AG, Germany) using a Plan-Apochromat 63×/1.4 Oil DIC M27 lens and 488- and 561-nm laser lines. Image acquisition, reconstruction, and alignment for structured illumination microscopy were performed using the Zeiss ZEN 2012 SP1 software (black edition, version 8.1.5.484). Contrast and colors were adjusted using ICY bioimage analysis software.

Small interfering RNA

Cells were irradiated and, after 24 h, plated into six-well dishes to form progeny colonies. After 24 h, these progeny colonies were transfected according to the manufacturer's instructions with "SMARTpool-siGENOME EPHA4 siRNA" or "Silencer® Select Negative Control siRNA," both at a final concentration of 5 nM. After transfection, cells were incubated for 48 h and the subsequent experiments were performed.

Invasion and transmigration assays

Control and irradiated cells (3×10^4) were seeded in FBS-free medium in the upper surface of the 8-μm pore Polycarbonate Membrane Transwell® Inserts (Costar Cambridge, MA) that were coated with 30 μl of Matrigel® (BD Biosciences) or uncoated for invasion or migration assays, respectively. DMEM with 10 % FBS was added as a chemoattractant in the lower chamber. After 24 h of incubation, the upper surface of the membrane was scrubbed. Cells in the lower membrane were fixed with ethanol, stained with 1 % violet crystal, analyzed under a microscope, and counted.

Statistical analysis

All quantitative data presented are the mean ± SEM from at least three independent experiments. Statistical analysis and the creation of graphs were performed using Prism 5.0 (GraphPad™ Software, San Diego, CA, USA). Student's t test was performed and differences were considered statistically significant when $p < 0.05$, $p < 0.01$, and $p < 0.001$.

Results

Progeny of HT-29 radiation survivor cells showed increased EphA4 activity

In our previous study, we showed that the progeny of irradiation survivor HT-29 cells develops a more aggressive phenotype [20]. To analyze the cell signaling pathways that support this phenotype, we initially investigated the activation levels of RTKs in these progeny colonies using the Human Phospho-RTK Array Kit. The F1 5Gy progeny showed an increase in activated EphA4 levels compared with F1 Cont (Fig. 1a). This result was confirmed by immunoprecipitation of EphA4 followed by immunoblotting with the anti-phosphotyrosine

antibody (Fig. 1b) and also by Western blotting using an antibody that recognizes specifically Tyr-602 EphA4 phosphorylation (Fig. 1c). Additionally, we observed no changes in the total EphA4 expression levels in F1 5Gy compared with F1 Cont (Fig. 1c).

The EphA4 pattern of distribution or the effect of radiation on its subcellular localization has never been investigated in CRC cells. Thus, using immunofluorescence, we showed that the distribution of EphA4 protein in F1 Cont cells is observed in both cell–cell contact regions and cytoplasmic labeling. The F1 5Gy progeny exhibited a similar distribution pattern, although it was more predominant in the cytoplasm (Fig. 1d) because this progeny does not exhibit well established cell–cell contacts [20].

EphA4 activation by the agonist doxazosin induced cell dispersion in CRC cells

Considering that EphA4 activation effects have never been investigated in CRC cells, we decided to analyze the effects of pharmacological EphA4 activation in HT-29 cells. Non-irradiated HT-29 (F1 Cont) cells were treated with the EphA4 agonist doxazosin to mimic the activation that was observed in F1 5Gy and evaluate whether the control progeny could display the same features of F1 5Gy. Originally developed as an antagonist for $\alpha 1$-adrenoreceptor, doxazosin is an approved drug (Cardura®) and was characterized as an agonist for EphA4 [23].

The IC_{50} dose of doxazosin for HT-29 cells was obtained by the MTT assay, and the IC_{20} (23 μM) was used in the subsequent experiments (Fig. 2a). EphA4 activation by doxazosin was confirmed through an activation kinetic assay using F1 Cont cell lysates and immunoblotting. We observed an increase in EphA4 activation in a time-dependent manner in F1 Cont cells treated for 5, 15, and 30 min with 23 μM doxazosin (Fig. 2b). In addition, phase-contrast microscopy images showed that F1 Cont cells treated with doxazosin for 24 h displayed a more dispersed pattern when compared with non-treated F1 Cont, where cells grew in well-delimited colonies (Fig. 2c). This result indicates that the activation of EphA4 by doxazosin could be involved in the disruption of cell–cell adhesion.

EphA4 activation by doxazosin induced adherens junction disorganization including E-cadherin internalization and downregulation

To investigate whether activation of EphA4 by doxazosin could modulate the adherens junctions, E-cadherin distribution and expression in the F1 Cont progeny treated with doxazosin were analyzed. We observed that E-cadherin was partially internalized and accumulated at perinuclear clusters in F1 Cont cells treated with doxazosin, although there is still

Fig. 1 Irradiation effects on the activity, expression, and subcellular localization of EphA4 in the progeny derived from irradiated cells. **a** Total cell lysates from HT-29 F1 Cont and F1 5Gy were obtained and analyzed using a Phospho-RTK Array kit. The array coordinates are shown on the *left side of the figure*, illustrating the localization of the spots containing immobilized antibodies. The *graph* on the *right side of the figure* depicts the quantification of the spots in the Phospho-RTK Array kit using a densitometry analysis. Data of a single experiment. **b** Total lysates from HT-29 F1 Cont and F1 5Gy cells were obtained and immunoprecipitated using an EphA4 antibody. The immunoprecipitates were analyzed by Western blot for phosphotyrosine. *Bar graphs* show the relative amount of p-Tyr linked to EphA4 levels (where F1 Cont = 1). Data of a single experiment. **c** Western blot analysis of p-EphA4 (Tyr-602) and EphA4 protein levels in lysates derived from HT-29 F1 Cont and F1 5Gy. *Bar graphs* are plotted as the fold change of protein expression (where F1 Cont = 1). GAPDH protein was used as a loading control. Data are presented as the mean ± SEM of three independent experiments. Significance was determined using a *t* test. *$p < 0.05$; **$p < 0.01$; ***$p < 0.001$. **d** F1 Cont and F1 5Gy of HT-29 cells were grown on glass coverslips until colony formation and subjected to immunofluorescence analysis of EphA4. Images are representative of three independent experiments. The nucleus was stained with DAPI. *Scale bar*, 20 mm

some labeling of E-cadherin at cell–cell contacts (Fig. 3a). In addition, a reduction in E-cadherin expression levels after doxazosin treatment was observed by immunoblotting (Fig. 3b). These results show that EphA4 activation induced a disruption of adherens junctions with internalization and reduced expression of E-cadherin, which could favor cell dispersion. These events observed in F1 Cont cells treated with doxazosin confirm that this effect mimics, at least in part, the phenotype induced by radiation.

EphA4 interacted with E-cadherin in the progeny of radiation survivor cells

Some Eph family receptors could interact with E-cadherin [24]. Additionally, these receptors are endocytosed upon their activation, leading to cell repulsion and dispersion [25]. Our results showed that doxazosin causes EphA4 activation and E-cadherin internalization, but an interaction between Eph receptors and E-cadherin has never been described. To better resolve the localization of E-cadherin relative to p-EphA4 in F1 Cont and F1 5Gy progenies, we used structured illumination microscopy. E-cadherin immunofluorescence was used to define the location of adherens junctions. Some p-EphA4 was found precisely co-localized with E-cadherin at cell–cell contacts in F1 Cont cells. In turn, the F1 5Gy progeny showed cytoplasmic labeling for p-EphA4 and for E-cadherin, and the image merge showed co-localization spots for both proteins, indicating that E-cadherin and p-EphA4 could be internalized together (Fig. 4a).

To further investigate the association between EphA4 and E-cadherin, EphA4 was immunoprecipitated and subsequent E-cadherin expression was analyzed by immunoblotting. Figure 4b shows the presence of E-cadherin in
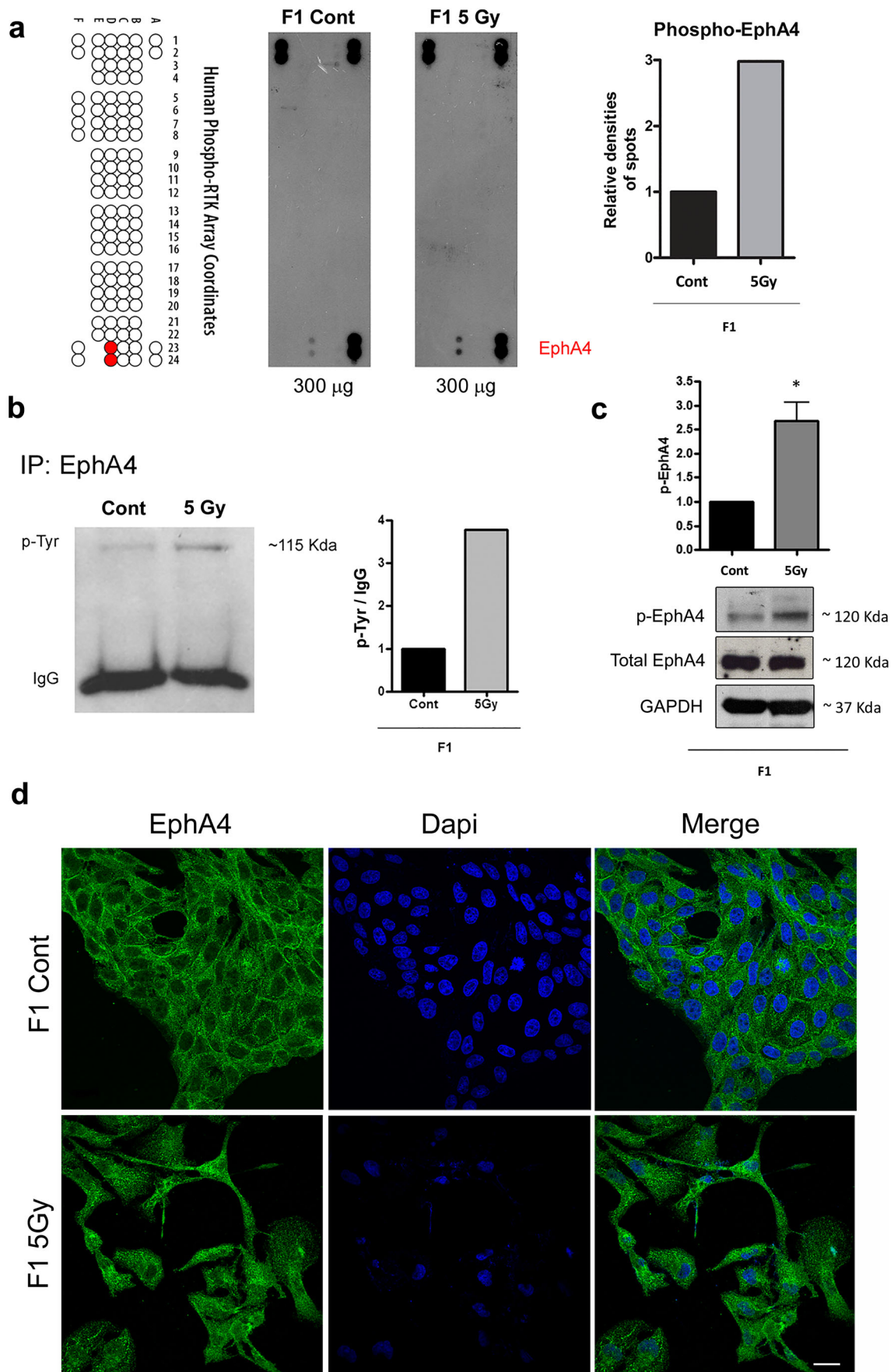
Fig. 2 Doxazosin activates EphA4 and induces cell dispersion in HT-29 CRC cells. **a** HT-29 cells (F1 Cont) were treated with doxazosin and cell viability was analyzed using the MMT methodology for IC$_{50}$ determination. *Graph* represents the percentage of viable cells as a function of doxazosin doses. **b** HT-29 cells were grown until subconfluence and treated with doxazosin for 5, 15, and 30 min, after which total cell lysates were analyzed using immunoblotting for EphA4 (Tyr-602) and total EphA4 levels. α-Tubulin was used as a loading control. *Numbers above the figure* represent the ratio of the optical density of doxazosin-treated to untreated cells (where non-treated cells = 1). **c** Cell morphology of the HT-29 F1 Cont treated with doxazosin for 24 h, as analyzed using phase-contrast microscopy. Images are representative of at least three experiments. *Scale bar*, 50 μm
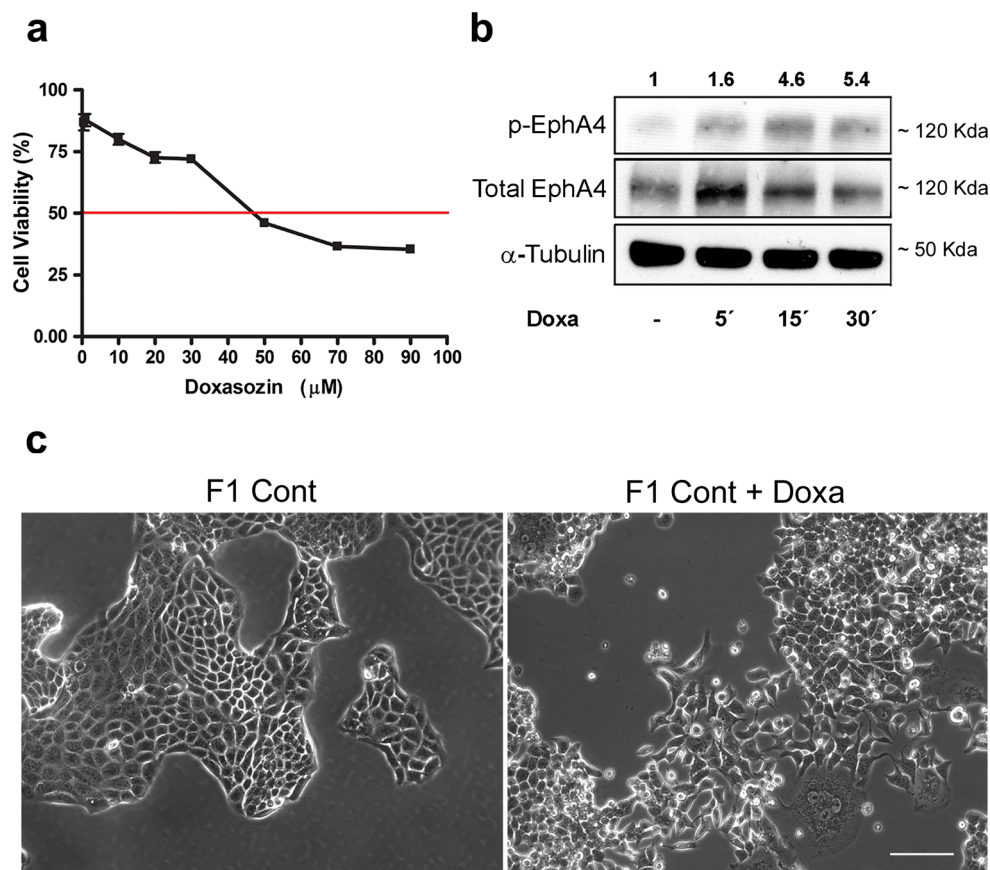
the EphA4-immunoprecipitated lysates, although there was no difference in E-cadherin–EphA4 association levels between F1 Cont and F1 5Gy in these lysates. We also showed that β-catenin immunoprecipitates with EphA4; thus, β-catenin might also be a target of EphA4 signaling, as suggested previously [26]. These results suggest that EphA4 and E-cadherin could be physically interacting.
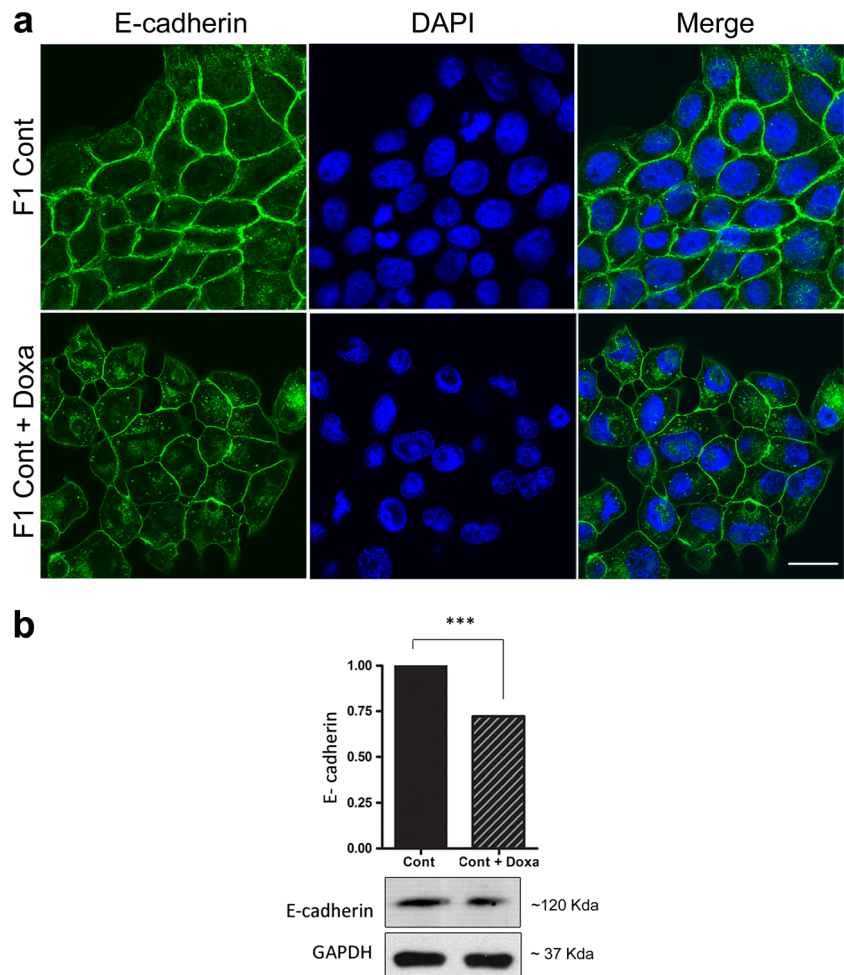
Promotion of migration, invasiveness, and metalloprotease-2 activity by EphA4 in the progeny of radiation survivor cells

To investigate whether EphA4 is essential for the aggressive phenotype displayed by the F1 5Gy progeny, EphA4 expression was silenced using small interfering RNA (siRNA). Figure 5a shows the high efficiency of EphA4 knockdown. Because F1 5Gy cells transfected with siRNA negative control showed no significant difference in EphA4 expression compared with F1 5Gy non-transfected cells, F1 5Gy non-transfected cells were used as a negative control in subsequent experiments. We found that EphA4 knockdown did not interfere with the colony formation capability of F1 5Gy cells (Fig. 5b), but this knockdown was able to reduce both the high migratory (Fig. 5c) and invasive (Fig. 5d) potential in this progeny. It was also able to reduce MMP-2 activity (Fig. 5e).

AKT and ERK1/2 signaling pathways were more active in the progeny of radiation survivor cells and ERK1/2 activation is dependent on EphA4

To explore additional signaling pathways in the F1 5Gy progeny, we evaluated its kinase activation profile using a Phospho-Kinase Array kit. Figure 6a shows increases in the phosphorylation levels of AKT, ERK1/2, GSK3, and β-catenin compared with the F1 Cont progeny. The increased levels of p-GSK3 (Ser9) and p-β-catenin corroborate the activation of the Wnt/β-catenin pathway in the F1 5Gy progeny that we showed in our previous study [20]. The increased levels of p-AKT and p-ERK1/2 were confirmed using immunoblotting (Supplemental Fig. 1). There is consistent evidence that PI3K/AKT and EKR1/2 regulate EMT-related events, such as metalloprotease expression/activity and increased expression of Snail, an E-cadherin transcriptional repressor [27, 28]. ERK1/2 and AKT are also common downstream targets of various RTKs, including EphA4, as observed in glioma cells [16]. Thus, we analyzed whether EphA4 could regulate the high levels of p-ERK1/2 and p-AKT observed in F1 5Gy. Figure 6b shows that the knockdown of EphA4 could dramatically reduce the level of p-ERK1/2 but not p-AKT, indicating that ERK1/2 is a downstream target of EphA4. To further confirm the involvement of ERK1/2 and PI3K/AKT in the

Fig. 3 Subcellular localization and E-cadherin expression upon EphA4 activation by doxazosin in HT-29 cells. **a** F1 Cont of HT-29 cells were grown in glass coverslips until colony formation and treated or not with 23 μM doxazosin for 24 h. Then, cells were subjected to immunofluorescence analysis of E-cadherin. Images are representative of three independent experiments. The nucleus was stained with DAPI. *Scale bar*, 20 μm. **b** Immunoblotting analysis of E-cadherin protein levels in lysates derived from HT-29 F1 Cont cells treated or not with 23 mM doxazosin for 24 h. *Bar graphs* are plotted as a fold change of protein expression (where non-treated cells = 1). GAPDH protein was used as a loading control. Data are presented as the mean ± SEM of three independent experiments. Significance was determined using a *t* test. *$p < 0.05$; **$p < 0.01$; ***$p < 0.001$

PI3K/AKT and ERK1/2 signaling pathways are respectively involved with the high invasive and migratory potential of the radiation survivor progeny

To elucidate the signaling pathways that give support to the aggressive features of the F1 5Gy cells, such as their high migratory and invasive potentials [20], these cells were treated with MEK1/2 and PI3K inhibitors and their migration and invasion potentials were analyzed. Figure 7a shows that the isolated inhibition of the ERK1/2 pathway and the co-inhibition of both pathways, but not the isolated inhibition of PI3K/AKT, could reduce the high migratory potential of the F1 5Gy cells. Furthermore, only the inhibition of PI3K/AKT, but not ERK1/2, could reduce the invasive potential of the F1 5Gy progeny (Fig. 7b). In other words, ERK1/2 is responsible for the high migration potential, whereas AKT regulates the invasiveness of the F1 5Gy progeny. Taken together, these results show that ERK1/2 is a downstream kinase of EphA4

aggressive properties displayed by the F1 5Gy cells, we performed pharmacological inhibition of ERK1/2 and PI3K/AKT (Fig. 6c).

and that the PI3K/AKT and ERK1/2 signaling pathways play an essential role in the high migratory and invasive potentials of the F1 5Gy progeny.

Discussion

CRC is one of the leading causes of cancer-related deaths worldwide, and the molecular mechanisms underlying its tumorigenesis are among the best characterized. The most supported model is the adenoma–carcinoma sequence, in which CRC arises through progressive accumulation of genetic and epigenetic mutations that confer the cells advantages and are clonally selected. The initiating events for the majority of CRCs are mutations in the *APC*, resulting in increased levels of β-catenin, followed by mutations in *K-ras* and in *p53* [29]. However, in a cohort of CRC patients, only 3.3 % of tumors contained the combination of these three gene mutations, suggesting that these mutations may lie on alternative pathways of tumor development in CRC [30]. RT is a common treatment for advanced rectal cancer and is a great benefit to many patients because it reduces the risk of local recurrence.

Fig. 4 Analysis of the interaction between EphA4 and E-cadherin in the progeny of radiation survivor cells. **a** HT-29 F1 Cont and F1 5Gy cells were grown on glass coverslips until colony formation and subjected to double labeling with E-cadherin and p-EphA4 (Tyr-602) and analyzed using super-resolution microscopy. Immunofluorescence localization of E-cadherin and p-EphA4, as detected using structured illumination microscopy, confirmed the co-localization of the proteins at the adherens junctions in F1 Cont and at the cytoplasm in F1 5Gy cells. *Scale bar*, 5 μm. **b** Total cell lysates from HT-29 F1 Cont and F1 5Gy were obtained and immunoprecipitated using EphA4 antibody. The immunoprecipitates were analyzed by Western blot for E-cadherin and β-catenin expression
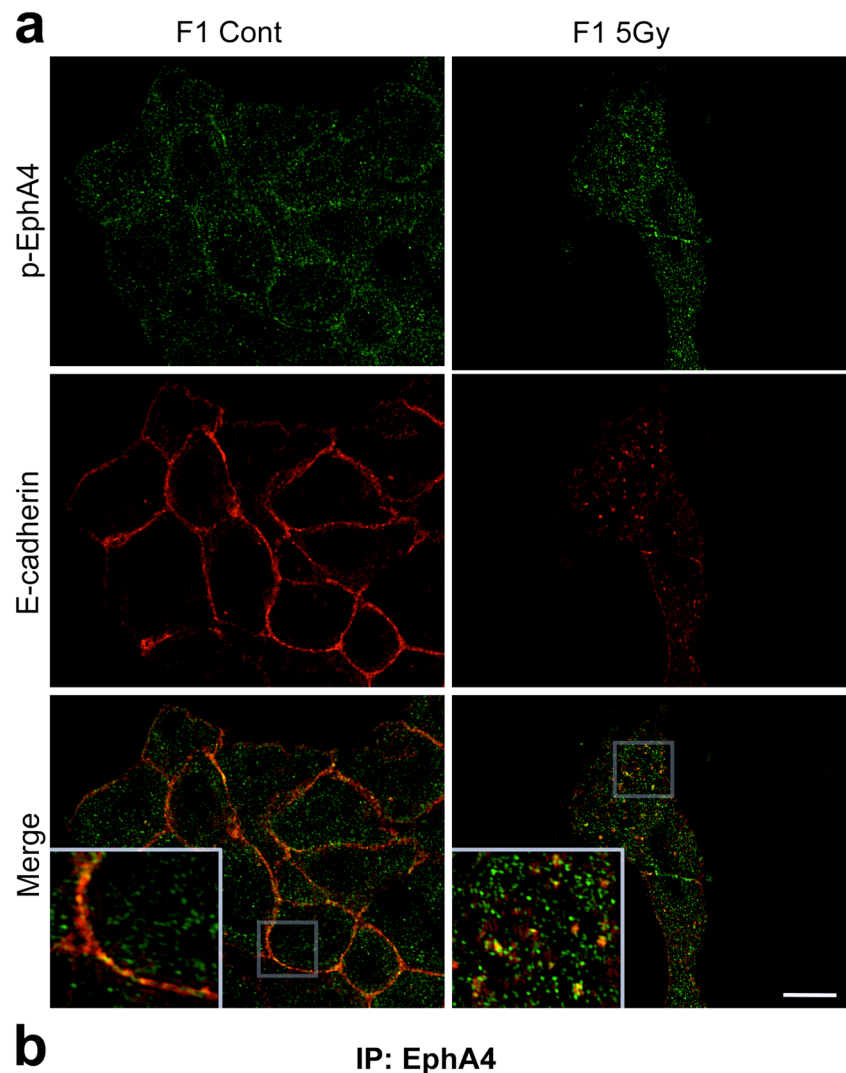
However, tumor relapses after RT tend to be more aggressive and are associated with poor prognosis. The ability of the cells to survive, invade, and generate a distant metastasis is the major cause of RT failure. Additionally, therapeutic stress caused by RT induces a strong release of growth factors and cytokines that not only control the normal tissue repair program but also induce the activation of signaling pathways favoring an aggressive phenotype of the remaining cells [10].

Increased EphA4 expression/activity has been reported in various types of cancers, including CRC, and its upregulation
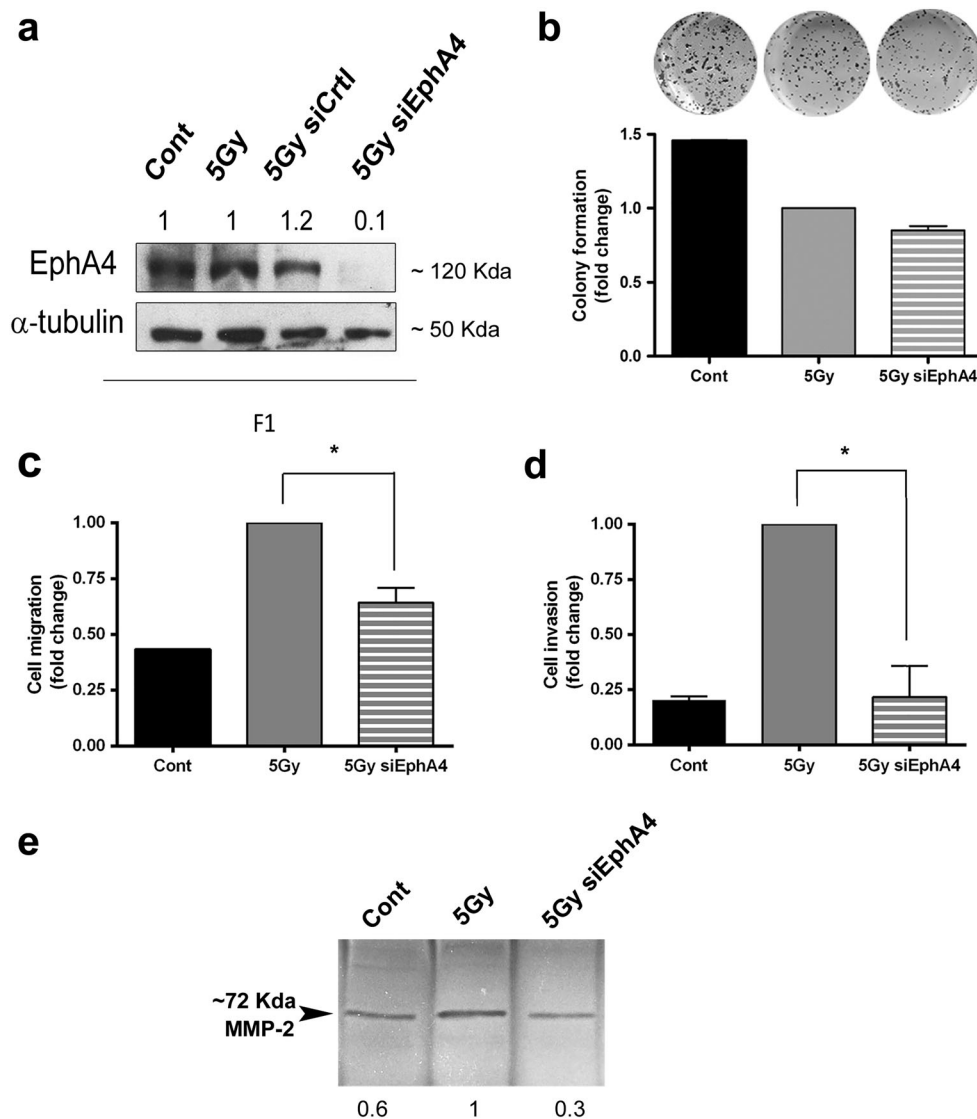
Fig. 5 Effects of EphA4 silencing on the malignant potential of the F1 5Gy progeny. **a** Immunoblotting analysis of EphA4 protein levels in lysates derived from HT-29 F1 Cont and F1 5Gy after 48 h of transfection with siRNA for EphA4. *Numbers above the figure* represent the ratio of the optical density of the bands as fold change of protein expression normalized by α-tubulin (where F1 Cont cells = 1). **b** Representative images of the clonogenic assay of HT-29 F1 Cont and F1 5Gy silenced or not for EphA4. *Bar graphs* are plotted as the fold change of colony formation after an optical density measurement at 595 nm for the eluate (where F1 5Gy = 1). Data are presented as the mean ± SEM of two independent experiments. **c, d** HT-29 F1 Cont and F1 5Gy silenced or not for EphA4 were plated in Boyden chambers, uncoated or coated with Matrigel, and subjected to migration (**c**) or invasion (**d**) assays, respectively. *Bar graphs* are plotted as the fold increase of cell migration or invasion (where F1 5Gy = 1). Data are presented as the mean ± SEM of three independent experiments. Significance was determined using a t test, *$P < 0.05$. **e** Conditioned culture media of HT-29 F1 Cont and F1 5Gy silenced or not for EphA4 were subjected to a zymography assay. The gel was scanned and the image was converted to black and white for the quantification of gel bands. *Numbers above the figure* represent the ratio of the optical density of the bands as fold change of metalloprotease activity (where F1 Cont cells = 1)

contributes to malignant events in several tumors [31]. However, the signaling mediated by this receptor has never been associated with a radioresponse, and its role in CRC remains largely unclear. Our results revealed high levels of activated EphA4 in the F1 5Gy progeny, which showed a highly aggressive EMT-like phenotype [20]. In this context, the only study that associates the Eph system with irradiation showed an increase in ephrin-A1 expression in radioresistant,

but not radiosensitive, squamous carcinoma cells after gamma radiation [32]. Next, we investigated the effect of EphA4 activation in CRC cells by using doxazosin in order to mimic some of the features of the F1 5Gy progeny, such as E-cadherin downregulation and altered subcellular localization [20]. We showed that doxazosin induced cell dispersion and partial internalization and reduced the expression of E-cadherin. Accordingly, EphA4 activation reduced E-cadherin
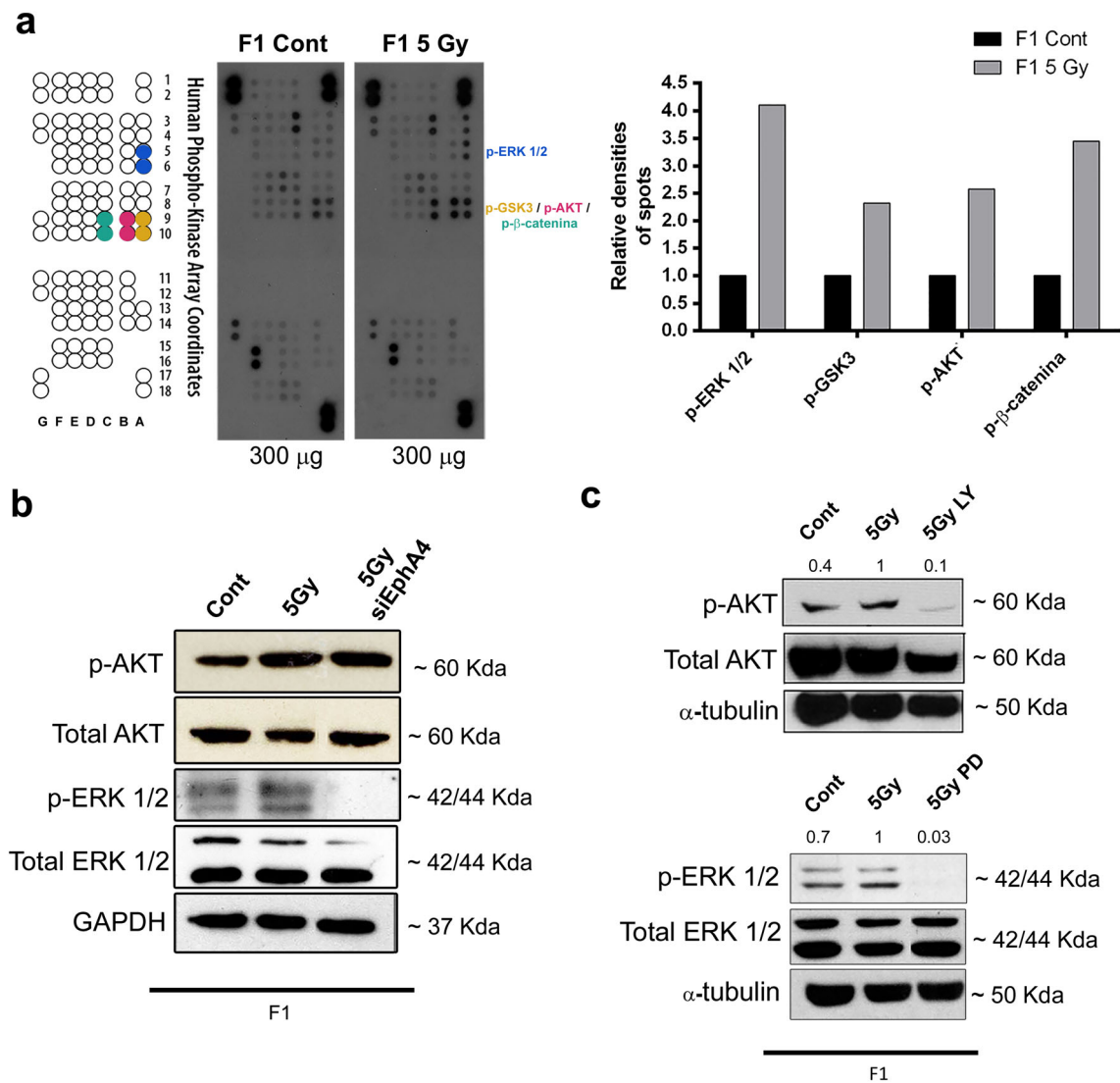
Fig. 6 Analysis of EphA4 downstream signaling pathways that contribute to the malignant potential in F1 5Gy progeny. **a** Total cell lysates from HT-29 F1 Cont and F1 5Gy were obtained and analyzed using a Phospho-Kinase Array kit. The array coordinates shown on the *left side of the figure* depict the localization of the spots containing immobilized antibodies on the nitrocellulose membrane. Spots A5 and A6 represent ERK1/2, spots C9 and C10 represent GSK3, spots B9 and B10 represent AKT, and spots A9 and A10 represent β-catenin. The *graph on the right side of the figure* depicts the quantification of the spots using densitometry analysis. **b** Immunoblotting analysis of p-ERK and p-AKT protein levels in lysates derived from HT-29 F1 Cont and F1 5Gy silenced or not for EphA4 after 48 h of transfection with siRNA. **c** Immunoblotting analysis of protein levels in lysates derived from HT-29 F1 Cont, F1 5Gy, and F1 5Gy treated with PI3K (LY294002) and MEK1/2 (PD98059) inhibitors. In (**c**), *numbers above the figure* represent the ratio of the optical density of the bands as a fold change of protein expression normalized to α-tubulin (where F1 5Gy cells = 1)

expression, mediating EMT in hepatoma cells [17], induced the loss of adherens junctions and polarity in *Xenopus* embryo [26], and increased the expression of Snail [33]. In agreement, our previous study showed an upregulation of Snail mRNA in the F1 5Gy progeny [20]. Together, these results indicate that in addition to inducing E-cadherin internalization, EphA4 could also reduce E-cadherin expression on a transcriptional level through Snail.

Some studies suggest regulation between E-cadherin and Eph receptors via a reciprocal regulatory mechanism because E-cadherin-dependent cell adhesion could regulate the expression, localization, and activation of these receptors [34, 35]. Furthermore, E-cadherin may be required for the membrane localization of Eph receptors [36]. In this context, EphA2 function is dependent on E-cadherin, but no evidence on an interaction between them was demonstrated [37]. Moreover, EphB/ephrin-B signaling regulates the formation of E-cadherin-based adhesions [38]. Here, for the first time, we show a direct interaction between EphA4 and E-cadherin (Fig. 4). EphA4 activation may be succeeded by its
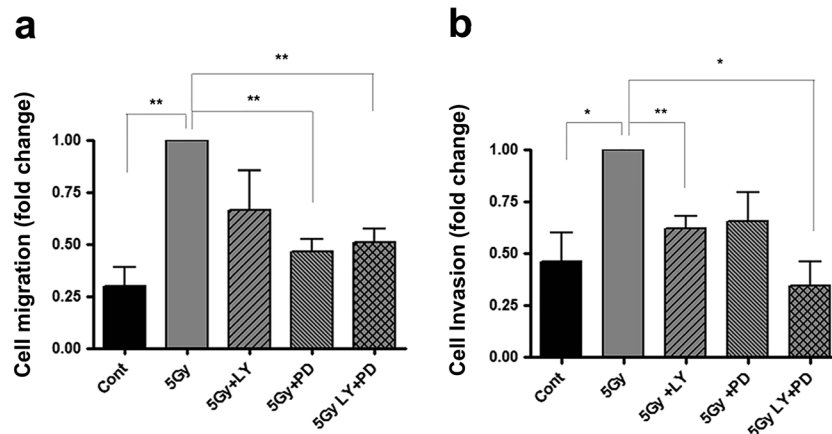
Fig. 7 Effects of PI3K and MEK inhibitors on the migratory and invasive potentials of the progeny derived from irradiated cells. **a**, **b** HT-29 F1 Cont, F1 5Gy, and F1 5Gy cells treated with the corresponding inhibitors were plated into Boyden chambers, uncoated (**a**) or coated with Matrigel (**b**), and subjected to migration or invasion assays, respectively. *Bar graphs* are plotted as the fold increase of cell migration or invasion (where F1 5Gy = 1). Data are presented as the mean ± SEM of triplicate assays for each cell line of three independent experiments. Significance was determined using a *t* test *$p < 0.05$; **$p < 0.01$

internalization, which is a well-known mechanism of Eph receptors and other RTKs [19]. Their direct interaction may cause E-cadherin internalization and possible degradation via proteasome, or downregulation at a transcriptional level leading to cell–cell adhesion loss, contributing to a more malignant potential.

To investigate whether EphA4 activation is involved with the malignant properties observed in the F1 5Gy progeny [17], we silenced this receptor and observed a reduction in the migratory and invasive potentials, and reduced MMP-2 activity, indicating that EphA4 contributes to this aggressive phenotype. Accordingly, EphA4 regulates MMP-2 activity in pancreatic cells [33] and the dissemination of prostate cancer cells via Vav2-RhoA [39]. Moreover, because its overexpression correlated with liver metastasis in CRC, EphA4 may be a potential metastasis biomarker [40].

After analyzing a broad spectrum of intracellular kinases, upregulation of p-AKT, p-ERK, p-β-catenin, and p-GSK3 (Ser9) was observed in the F1 5Gy progeny. We also showed that ERK1/2 activation is dependent on EphA4. MAPK activation by EphA4 was also observed in glioma and prostate cancer, but not in CRC cells [16, 41]. Because the p-AKT level in the F1 5Gy progeny was not altered by EphA4 knockdown, it is likely that other signaling pathways induced by radiation could activate it. The role of PI3K/AKT and ERK1/2 in the first stages of tumor development is well understood, but little is known about their effect during the late stages of tumor progression and after infrared treatment. The activation of PI3K/AKT and ERK1/2 can be induced by therapy stress and can trigger an adaptive response related to cell invasion through altered interconnected pathways [10]. Our results show that PI3K/AKT and ERK1/2 play an important role in coordinating the aggressive features displayed by the F1 5Gy progeny and suggest that these pathways could be responsible for therapy failure in CRC patients.

In summary, our results demonstrated that radiation induced EphA4 activation in the progeny of cells submitted to this treatment. This activation caused adherens junction disorganization and, consequently, cell dispersion. Furthermore, EphA4 activates ERK1/2 as a downstream pathway, and along with PI3K, EphA4 coordinates cell migration and invasion. These cellular events could be responsible for the high rates of therapeutic failure in inhibiting local invasion and metastasis in rectal cancer after radiotherapy. Because RTKs are surface molecules and therefore promising "druggable" targets, the inhibition of EphA4 could be an interesting strategy in adjuvant RT in CRC patients to reduce the therapeutic failure rates caused by local invasion and metastasis formation.

References

1. Torre LA, Bray F, Siegel RL, Ferlay J, Lortet-Tieulent J, Jemal A. Global cancer statistics, 2012. CA Cancer J Clin. 2015;65(2):87–108.

2. Instituto Nacional de Câncer José Alencar Gomes da Silva; Ministério da Saúde. Estimativa 2014. 2013; Rio de Janeiro.

3. Glynne-Jones R, Hadaki M, Harrison M. The status of targeted agents in the setting of neoadjuvant radiation therapy in locally advanced rectal cancers. J Gastrointest Oncol. 2013;4(3):264–84.

4. Sauer R, Becker H, Hohenberger W, Rödel C, Wittekind C, German Rectal Cancer Study Group, et al. Preoperative versus postoperative chemoradiotherapy for rectal cancer. N Engl J Med. 2004;351(17):1731–40.

5. Colorectal Cancer Collaborative Group. Adjuvant radiotherapy for rectal cancer: a systematic overview of 8,507 patients from 22 randomised trials. Lancet. 2001;358(9290):1291–304.

6. Madani I, de Neve W, Mareel M. Does ionizing radiation stimulate cancer invasion and metastasis? Bull Cancer. 2008;95(3):292–300.

7. Vicini F, Kestin L, Huang R, Martinez A. Does local recurrence affect the rate of distant metastases and survival in patients with early-stage breast carcinoma treated with breast-conserving therapy? Cancer. 2003;97(4):910–9.

8. van den Brink M, Stiggelbout AM, van den Hout WB, Kievit J, Klein Kranenbarg E, et al. Clinical nature and prognosis of locally recurrent rectal cancer after total mesorectal excision with or without preoperative radiotherapy. J Clin Oncol. 2004;22:3958–64.

9. Prise K, Schettino G, Folkard M. New insights on cell death from radiation exposure. Lancet Oncol. 2005;6(7):520–8.

10. Alexander S, Friedl P. Cancer invasion and resistance: interconnected processes of disease progression and therapy failure. Trends Mol Med. 2012;18:13–26.

11. Yacoub A, Miller A, Caron RW, Qiao L, Curiel DA, et al. Radiotherapy-induced signal transduction. Endocr Relat Cancer. 2006;13:S99–114.

12. Motzer RJ, Escudier B, Oudard S, Hutson TE, Porta C, RECORD-1 Study Group, et al. Phase 3 trial of everolimus for metastatic renal cell carcinoma: final results and analysis of prognostic factors. Cancer. 2010;116(18):4256–65.

13. Yao JC, Shah MH, Ito T, Bohas CL, Wolin EM, et al. Everolimus for advanced pancreatic neuroendocrine tumors. N Engl J Med. 2011;364(6):514–23.

14. Kullarnder K, Klein R. Mechanisms and functions of Eph and ephrin signaling. Nat Rev Mol Cell Biol. 2002;7:475–86.

15. Fox BP, Kandpal RP. Invasiveness of breast carcinoma cells and transcript profile: Eph receptors and ephrin ligands as molecular markers of potential diagnostic and prognostic application. Biochem Biophys Res Commun. 2004;318(4):882–92.

16. Fukai J, Yokote H, Yamanaka R, Arao T, Nishio K, Itakura T. EphA4 promotes cell proliferation and migration through a novel EphA4-FGFR1 signaling pathway in the human glioma U251 cell line. Mol Cancer Ther. 2008;7(9):2768–78.

17. Yan Y, Luo YC, Wan HY, Wang J, Zhang PP, et al. MicroRNA-10a is involved in the metastatic process by regulating Eph tyrosine kinase receptor A4-mediated epithelial-mesenchymal transition and adhesion in hepatoma cells. Hepatology. 2013;57(2):667–77.

18. Takano H, Nakamura T, Tsuchikawa T, Kushibiki T, Hontani K, et al. Inhibition of Eph receptor A4 by 2,5-dimethylpyrrolyl benzoic acid suppresses human pancreatic cancer growing orthotopically in nude mice. Oncotarget. 2015;6(38):41063–76.

19. Pasquale EB. Eph receptors and ephrins in cancer: bidirectional signalling and beyond. Nat Rev Cancer. 2010;10(3):165–80.

20. Bastos LG, de Marcondes PG, de-Freitas-Junior JC, Leve F, Mencalha AL, et al. Progeny from irradiated colorectal cancer cells acquire an EMT-like phenotype and activate Wnt/β-catenin pathway. J Cell Biochem. 2014;115(12):2175–87.

21. Flatmark K, Maelandsmo GM, Martinsen M, Rasmussen H, Fodstad Ø. Twelve colorectal cancer cell lines exhibit highly variable growth and metastatic capacities in an orthotopic model in nude mice. Eur J Cancer. 2004;40:1593–8.

22. Rowan AJ, Lamlum H, Ilyas M, Wheeler J, Straub J, Papadopoulou A, et al. APC mutations in sporadic colorectal tumors: a mutational "hotspot" and interdependence of the "two hits". Proc Natl Acad Sci U S A. 2000;97:3352–7.

23. Petty A, Myshkin E, Qin H, Guo H, Miao H, et al. A small molecule agonist of EphA2 receptor tyrosine kinase inhibits tumor cell migration in vitro and prostate cancer metastasis in vivo. PLoS One. 2012;7(8):e42120.

24. Kandouz M. The Eph/Ephrin family in cancer metastasis: communication at the service of invasion. Cancer Metastasis. 2012;31(1–2):353–73.

25. Nievergall E, Lackmann M, Janes P. Eph-dependent cell-cell adhesion and segregation in development and cancer. Cell Mol Life Sci. 2011;11:1813–42.

26. Winning R, Wyman T, Walker G. EphA4 activity causes cell shape change and a loss of cell polarity in Xenopus laevis embryos. Differentiation. 2001;68(2–3):126–32.

27. Campbell P, Channing J. Oncogenic Ras and its role in tumor cell invasion and metastasis. Semin Cancer Biol. 2004;14(2):105–14.

28. Grille S, Bellacosa A, Upson J, Klein-Szanto AJ, van Roy F, et al. The protein kinase Akt induces epithelial mesenchymal transition and promotes enhanced motility and invasiveness of squamous cell carcinoma lines. Cancer Res. 2003;63(9):2172–8.

29. Anwar M, Kochhar R, Singh R, Bhatia A, Vaiphei K. Frequent activation of the β-catenin gene in sporadic colorectal carcinomas: a mutational & expression analysis. Mol Carcinog. 2015. doi:10.1002/mc.22414.

30. Malhotra P, Anwar M, Nanda N, Kochhar R, Wig JD. Alterations in K-ras, APC and p53-multiple genetic pathway in colorectal cancer among Indians. Tumour Biol. 2013;34(3):1901–11.

31. Liizumi M, Hosokawa M, Takehara A, Chung S, Nakamura T, et al. EphA4 receptor, overexpressed in pancreatic ductal adenocarcinoma, promotes cancer cell growth. Cancer Sci. 2006;97(11):1211–6.

32. Nojiri K, Iwakawa M, Ichikawa Y, Imadome K, Sakai M, et al. The proangiogenic factor ephrin-A1 is up-regulated in radioresistant murine tumor by irradiation. Exp Biol Med. 2009;234(1):112–22.

33. Liu C, Huang H, Wang C, Kong Y. Involvement of ephrin receptor A4 in pancreatic cancer cell motility and invasion. Oncol Lett. 2014;7(6):2165–9.

34. Arvanitis D, Davy A. Eph/ephrin signaling: networks. Genes Dev. 2008;22:416–29.

35. Ireton R, Chen J. EphA2 receptor tyrosine kinase as a promising target for cancer therapeutics. Curr Cancer Drug Targets. 2005;5:149–57.

36. Orsulic S, Kemler R. Expression of Eph receptors and ephrins is differentially regulated by E-cadherin. J Cell Sci. 2000;113:1793–802.

37. Zantek ND, Azimi M, Fedor-Chaiken M, Wang B, Brackenbury R, Kinch MS. E-cadherin regulates the function of the EphA2 receptor tyrosine kinase. Cell Growth Differ. 1999;10:629–38.

38. Solanas G, Cortina C, Sevillano M, Batlle E. Cleavage of E-cadherin by ADAM10 mediates epithelial cell sorting downstream of EphB signalling. Nat Cell Biol. 2011;13(9):1100–7.

39. Batson J, MacCarthy-Morrogh L, Archer A, Tanton H, Nobes CD. EphA receptors regulate prostate cancer cell dissemination through Vav2–RhoA mediated cell–cell repulsion. Biol Open. 2004;3(6):453–62.

40. Oshima T, Akaike M, Yoshihara K, Shiozawa M, Yamamoto N, et al. Overexpression of EphA4 gene and reduced expression of EphB2 gene correlates with liver metastasis in colorectal cancer. Int J Oncol. 2008;33(3):573–7.

41. Shin J, Gu C, Kim J, Soochul P. Transient activation of the MAP kinase signaling pathway by the forward signaling of EphA4 in PC12 cells. BMP Rep. 2008;41(6):479–84.